

Effect of Vibrational Excitation on the Collisional Removal of Free Radicals by Atoms: OH($\nu=1$) + N

Ani Khachatryan and Paul J. Dagdigian*

Department of Chemistry, The Johns Hopkins University, Baltimore, Maryland 21218-2685

Received: October 24, 2005; In Final Form: January 18, 2006

The collisional removal of vibrationally excited OH($\nu=1$) by N(4S) atoms is investigated. The OH radical was prepared by 193 nm photolysis of H₂O₂, and N(4S) atoms were generated by a microwave discharge in N₂ diluted in argon. The concentrations of OH($\nu=0$ and 1) were monitored by laser-induced fluorescence as a function of the time after the photolysis laser pulse. The N(4S) concentration was determined from the OH($\nu=0$) decay rate, using the known rate constant for the OH($\nu=0$) + N(4S) \rightarrow H + NO reaction. From comparison of the OH($\nu=0$ and 1) decay rates, the ratio of the rate constant $k_{\nu=1}(\text{OH-N})$ for removal of OH($\nu=1$) in collisions with N(4S) and the corresponding OH($\nu=0$) rate constant, $k_{\nu=0}(\text{OH-N})$ was determined to be 1.61 ± 0.42 , yielding $k_{\nu=1}(\text{OH-N}) = (7.6 \pm 2.1) \times 10^{-11} \text{ cm}^3 \text{ molecule}^{-1} \text{ s}^{-1}$, where the quoted uncertainty (95% confidence limits) includes the uncertainty in $k_{\nu=0}(\text{OH-N})$. Thus, the collisional removal of OH($\nu=1$) by N(4S) atoms is found to be faster than for OH($\nu=0$).

1. Introduction

The hydroxyl (OH) radical is an important intermediate in combustion and in the chemistry of the lower and upper atmospheres. Knowledge of the rate constants for reactions involving the hydroxyl radical is very important for an understanding of this chemistry, and much effort has gone into the measurement of these rate constants.^{1,2} Similarly, there has been considerable interest in the rates of collisional vibrational relaxation of OH in its ground X² Π electronic state. In part, this has been driven by the need to understand quantitatively the intensity and vibrational distribution of the emission of OH in the upper atmosphere.^{3–5} There has been a number of studies of the collisional vibrational relaxation of OH(X² Π) in a wide range of vibrational levels by stable collisional partners.^{6–17}

There has also been some study of the vibrational relaxation of OH by open-shell species. Of particular interest is the relaxation of OH(ν) by oxygen atoms because they are present in significant concentrations in the upper atmosphere. The collisional removal of OH($\nu \geq 1$) by O(³P) has been studied both experimentally^{18–20} and theoretically.²¹ In the course of a study of the reaction of vibrationally excited water with hydrogen atoms, Barnes et al.²² measured the rate constant for relaxation of OH($\nu=1$) by H atoms. Atahan and Alexander²³ have applied a quantum statistical capture model, which was developed by Manolopoulos and co-workers^{24–26} and later extended²⁶ to include all couplings prior to formation of the complex, to the collisional vibrational relaxation of OH($\nu=1$ and 2) by H atoms.

Our expectations for the collision dynamics and the dependence upon the vibrational quantum number of a vibrationally excited open-shell species such as OH with closed-shell and open-shell collision partners are quite different. The rate constant for collisional vibrational relaxation of OH($\nu=1$) by O₂ was recently reported to equal $(0.75 \pm 0.22) \times 10^{-13} \text{ cm}^3 \text{ molecule}^{-1} \text{ s}^{-1}$.¹⁷ The total rate constant for removal of OH(ν) by O₂ is found to increase monotonically with vibrational quantum number up to a value of $(2.79 \pm 0.14) \times 10^{-11} \text{ cm}^3 \text{ molecule}^{-1} \text{ s}^{-1}$ for $\nu = 11$.¹² This behavior is consistent with the linear

dependence on ν predicted by simple theories of vibrational energy transfer,²⁷ which apply to the primarily repulsive interactions between closed-shell molecules that lead to vibrational-to-translational energy transfer.

By contrast, interactions of two open-shell species will involve more than one potential energy surface (PES). For many such systems, at least one of these PESs will be strongly attractive, with no barrier at long range. In a collisional encounter, the reagents can combine on this attractive PES to form a transient complex that subsequently dissociates at low pressures. For systems in which the complex can only redissociate back to the reagents, the transient complex can be collisionally stabilized at very high pressures, leading to association. As discussed by Smith,²⁸ the high-pressure limit of the association rate would be expected to equal the rate of vibrational relaxation in such systems. Both processes should equal the rate of formation of the complex if the reagents interact through a strongly attractive PES such that the rate of formation of the transient complex is independent of the initial vibrational quantum number. This relationship is found to be approximately true in a number of systems.²⁸ Another corollary is that the rate of vibrational relaxation should be independent of ν if the rate of formation is independent of the vibrational level of the diatom. The rate of vibrational relaxation appears to be independent of ν for relaxation of NO(ν) by O(³P) atoms.^{29–31} In their theoretical study of OH(ν)-H collisions, Atahan and Alexander²³ found that the 300 K rate constant for vibrational relaxation for $\nu = 2$ is only 6% higher than that for $\nu = 1$.

In the case of the interaction of OH with O(³P) and N(4S) atoms, the reagents can combine on one or more attractive PESs to form a transient complex (HO₂ and HNO/HON, respectively). These systems differ from those involving two open-shell reagents discussed above in that these complexes can also decompose by chemical reaction, forming H + O₂ and H + NO, respectively, as well as by redissociation back to reagents. Moreover, the binding energies of the complexes are somewhat smaller than for a normal chemical bond. Experimental^{19,20} and theoretical²¹ studies suggest that the total removal rate constant

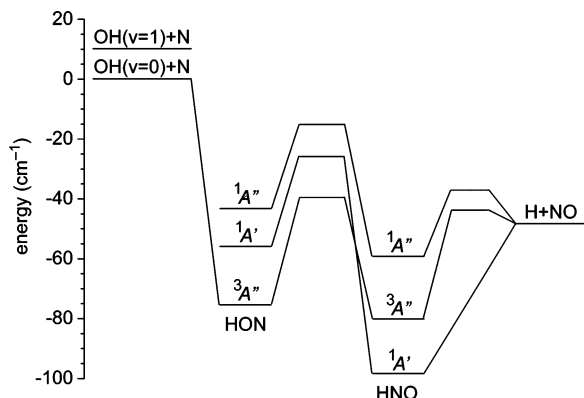
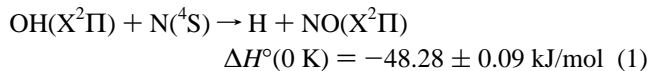


Figure 1. Schematic energy diagram for the $\text{OH}(\text{X}^2\Pi) + \text{N}(\text{S}^4) \rightarrow \text{H} + \text{NO}(\text{X}^2\Pi)$ reaction. Energies of the HON and HNO complexes and of the transition states were taken from ref 34. The pathways for dissociation of HON to $\text{H} + \text{NO}(\text{X}^2\Pi)$ are not explicitly included. The singlet surfaces do not connect with the $\text{OH}(\text{X}^2\Pi) + \text{N}(\text{S}^4)$ asymptote.

for $\text{OH}(\nu \geq 1)$ in collisions with $\text{O}(\text{P}^3)$ is moderately larger than that for $\text{OH}(\nu = 0)$. In a recent study,²⁰ we investigated the collisional removal of $\text{OH}(\nu = 1)$ by $\text{O}(\text{P}^3)$ through comparison of the rate of decay of $\text{OH}(\nu = 0$ and 1) in the presence of $\text{O}(\text{P}^3)$ atoms. We found that the ratio of the total removal rate constants for $\text{OH}(\nu = 1)$ vs $\text{OH}(\nu = 0)$ was 1.1 ± 0.1 . Hence, the collisional removal of $\text{OH}(\nu = 1)$ is slightly faster than for $\text{OH}(\nu = 0)$, but the difference in the rate constants is within the experimental uncertainty. It would thus be interesting to investigate other systems of two open-shell reagents to see if the total removal rate constants depend on the reagent diatomic vibrational quantum number.

The present paper presents a study of the relaxation of $\text{OH}(\nu = 1)$ through collisions with $\text{N}(\text{S}^4)$ atoms. The OH ground vibrational level can be removed in collisions with nitrogen atoms through the reaction



The enthalpy of reaction 1 was computed from heats of formation from the JANAF thermochemical tables³² and Ruscic et al.³³ There is also a third chemical channel in this system, namely, $\text{O}(\text{P}^3) + \text{NH}(\text{X}^3\Sigma^-)$, which lies at significantly higher energy and is hence not relevant here. Guadagnini et al.³⁴ have carried out an extensive ab initio study of PESs connecting these chemical channels. As illustrated in Figure 1, the $\text{OH}(\text{X}^2\Pi)$ and $\text{N}(\text{S}^4)$ reagents can interact without a barrier on a ${}^3\text{A}''$ PES to form a HON complex, which can isomerize to form HNO and then dissociate to $\text{H} + \text{NO}(\text{X}^2\Pi)$ products. The HON complex is computed³⁴ to be bound by 305 kJ/mol with respect to $\text{OH}(\text{X}^2\Pi) + \text{N}(\text{S}^4)$. The other PESs (${}^3\text{A}'$, ${}^5\text{A}'$, ${}^5\text{A}''$) are not attractive in the entrance channel and are not involved in reaction 1.

The rate constant for reaction 1 has been measured over a range of temperatures in several studies.^{35–37} Howard and Smith³⁵ report a room-temperature rate constant $k_{\nu=0}(\text{OH}-\text{N}) = (4.74 \pm 0.44) \times 10^{-11} \text{ cm}^3 \text{ molecule}^{-1} \text{ s}^{-1}$ for reaction 1; Smith and Stewart³⁶ report a slightly higher value for this rate constant, $(5.2 \pm 0.3) \times 10^{-11} \text{ cm}^3 \text{ molecule}^{-1} \text{ s}^{-1}$. Smith and co-workers³⁸ have determined the nascent vibrational state distribution of the NO product from reaction 1. Several theoretical studies of reaction 1 have been carried out on the basis of the PESs computed by Guadagnini et al.³⁴ Schatz and co-workers³⁹ have performed classical trajectory calculations of collisions of all three possible atom–diatom arrangements of the HNO system. Of relevance to this work, they computed

the thermal rate constant for reaction 1 at several temperatures and NO product vibrational state distribution. The calculated room-temperature rate constant is slightly lower than the experimental value reported by Howard and Smith,³⁵ and the NO product vibrational state distribution is in reasonable agreement with the experimental measurements by Smith et al.³⁸ Recently, Chen et al.⁴⁰ have carried out time-dependent quantum mechanical wave packet calculations of reaction 1 on the ${}^3\text{A}''$ PES. The calculated reaction cross sections are found to be a decreasing function of the translational energy, in agreement with the trajectory calculations.

2. Experimental Section

These experiments were carried out in the apparatus employed for our previous study of the vibrational relaxation of OH by oxygen atoms.²⁰ Nitrogen atoms were generated by passing a 5% mixture of N_2 in Ar at a total pressure of 2.2 Torr through a 2450 MHz microwave discharge (80 W). The gas mixture (120 sccm total, measured with calibrated flow meters) flowed at an estimated velocity of 150 cm/s through a 3.1×6.3 cm rectangular section mounted on a 1 m spectrometer, which was used with wide slits (4 nm spectral resolution) to isolate laser-induced fluorescence in a given vibrational band. All surfaces downstream of the discharge were coated with fluorocarbon wax to inhibit wall recombination. Pressures were measured with a capacitance manometer (MKS).

The photolytic OH precursor H_2O_2 was added (2.5 mTorr) neat through a Teflon needle valve 10 cm upstream of the laser fluorescence detection zone, and the H_2O_2 partial pressure was determined by monitoring the pressure rise in the system while opening the needle valve controlling the H_2O_2 flow. The partial pressures of the reagents were the same to ± 1 mTorr from run to run. Concentrated liquid H_2O_2 ($\geq 95\%$) was prepared by pumping on 30% reagent. The vapor above a 95% solution is estimated to be 90% H_2O_2 , with the remainder H_2O .⁴¹

Hydroxyl radicals were generated by 193 nm photolysis of H_2O_2 using laser radiation from a Lambda Physik COMPex 102 excimer laser. Typical photolysis laser energies were 10 mJ in a 1.2 cm diam beam in the flow apparatus. On the basis of the 193 nm absorption cross section and the quantum yields for the $\text{OH} + \text{OH}$ and $\text{H} + \text{HO}_2$ dissociation channels,¹ we estimate 0.8% dissociation of H_2O_2 and an initial OH concentration of $7 \times 10^{11} \text{ molecules cm}^{-3}$. H_2O_2 was deemed to be a more suitable precursor than the commonly employed HNO_3 precursor because the latter also yields $\text{O}(\text{D}^1)$ at 193 nm,^{42,43} which reacts with hydrogen-containing compounds to form $\text{OH}(\nu)$, causing a cascade contribution to the $\text{OH}(\nu = 1)$ concentration. Photolysis at 248 nm would provide a cleaner course of OH, but the absorption cross sections are too low² to allow detectable photolytic production of $\text{OH}(\nu = 1)$ at the low partial pressures of the precursor needed to minimize vibrational relaxation by the precursor.

$\text{OH}(\nu = 0$ and 1) were detected at a variable delay after photolysis by pulsed laser fluorescence excitation on the A–X (1,0) $\text{Q}_1(1)$ and (2,1) $\text{Q}_1(2)$ lines and detection in the (1,1) and (2,2) bands, respectively. The frequency-doubled output of a Continuum Sunlite EX optical parametric oscillator was employed for excitation. The probe beam counterpropagated along the photolysis laser beam and was introduced through the opposite sidearm of the apparatus. The delay between the photolysis and probe lasers was set by a digital delay generator that was controlled by the data acquisition computer. A data collection run consisted of recording the fluorescence intensity

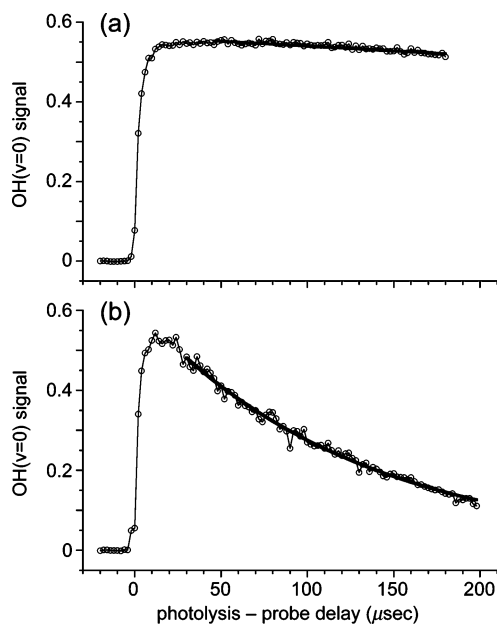


Figure 2. Time-dependent concentrations of $\text{OH}(v=0)$ as a function of the time between the photolysis and probe laser pulses, with the microwave discharge (a) off and (b) on. Partial pressures of the added reagents: Ar, 2.1; N_2 , 0.1 H_2O_2 , 0.0025 Torr. The displayed plots represent single data collection runs (see text). The heavy solid lines show least-squares fits of the decay profiles to exponential functions. The fitted decay rate for the plot in panel (b) was $(8.250 \pm 0.095) \times 10^3 \text{ s}^{-1}$, from which a $\text{N}(^4\text{S})$ concentration of $(1.617 \pm 0.032) \times 10^{14} \text{ atoms cm}^{-3}$ was derived (see text).

(10-shot average) while cycling through a grid of delays typically 20 times.

3. Results

The total removal rate constant $k_{v=1}(\text{OH}-\text{N})$ for collisions of $\text{OH}(v=1)$ with $\text{N}(^4\text{S})$ atoms was determined by analysis of the temporal decays of the $\text{OH}(v=0$ and 1) concentrations. Figure 2 presents the $\text{OH}(v=0)$ concentrations, measured by laser-induced fluorescence detection in single runs, with the microwave discharge off and on. In both cases, the concentrations are seen to build up initially, due to rotational thermalization, and then decrease at larger delays. The $\text{OH}(v=0)$ concentration with the discharge off is seen to decay very slowly, mainly from diffusion out of the laser excitation/detection zone. By contrast, the $\text{OH}(v=0)$ concentration decays more rapidly with the discharge on, due to reaction with $\text{N}(^4\text{S})$ atoms. As described below, the $\text{N}(^4\text{S})$ concentration was computed from the $\text{OH}(v=0)$ decay rate with the discharge on, using a literature value³⁵ for $k_{v=0}(\text{OH}-\text{N})$, the rate constant for the $\text{OH}(v=0) + \text{N}(^4\text{S})$ reaction.

Figure 3 presents a plot of the $\text{OH}(v=1)$ concentration, measured in a single run with the microwave discharge on, as a function of the photolysis–probe delay. It can be seen that the signal is much weaker, and hence noisier, than for $\text{OH}(v=0)$. This is due to the small ($\sim 1\%$) fraction of $\text{OH}(v=1)$ produced in the photolysis of H_2O_2 .^{44,45} The spike at $t = 0$ is due to scattered light from the excimer laser. The $k_{v=1}(\text{OH}-\text{N})$ rate constant was determined from the $\text{OH}(v=1)$ decay rate, taking into account the relaxation due to H_2O_2 and other species, and the $\text{N}(^4\text{S})$ concentration determined as described above.

It can be seen in Figure 2 that the $\text{OH}(v=0)$ signal intensity at short photolysis–probe delays does not change appreciably when the microwave discharge is turned on. We similarly observed no decrease in the $\text{OH}(v=1)$ signal at short photoly-

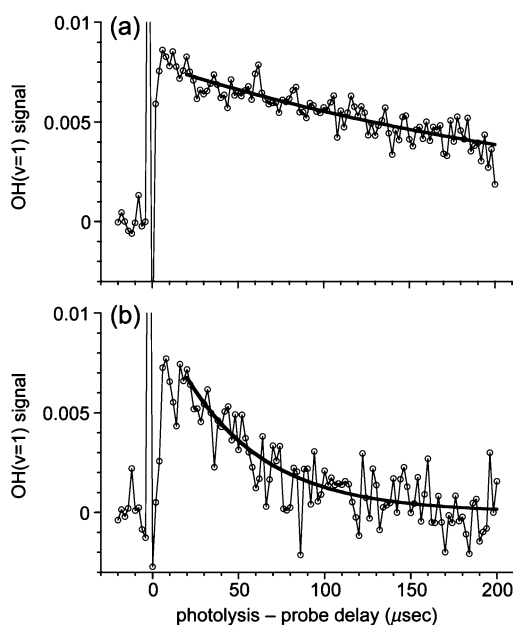


Figure 3. Time-dependent concentrations of $\text{OH}(v=1)$ as a function of the time between the photolysis and probe laser pulses, with the microwave discharge (a) off and (b) on. Partial pressures of the added reagents: Ar, 2.1; N_2 , 0.1 H_2O_2 , 0.0025 Torr. The displayed plot represents a single data collection run (see text). The heavy solid line shows a least-squares fit of the decay profile to an exponential function. The fitted decay rates were $(0.45 \pm 0.03) \times 10^4$ and $(2.11 \pm 0.21) \times 10^4 \text{ s}^{-1}$ for panels a and b, respectively.

sis–probe delay times when the microwave discharge was turned on. This contrasts with our observations²⁰ of OH photolytically produced from H_2O_2 in flows of $\text{O}(^3\text{P})$ atoms; in this system the $\text{OH}(v=0$ and 1) concentrations dropped by a factor of ~ 3 when the microwave discharge was turned on, reflecting the loss of the H_2O_2 precursor from a slow chain reaction involving $\text{O}(^3\text{P})$ atoms, HO_2 , OH , and H atoms in the time between the addition of H_2O_2 to the flow and the laser excitation/detection zone. In determining the total collisional removal rate of $\text{OH}(v=1)$ by $\text{O}(^3\text{P})$ atoms, we had to take into account the presence of free radical species generated in the decomposition of the H_2O_2 precursor.²⁰ A similar loss of H_2O_2 does not occur in flows of $\text{N}(^4\text{S})$ because these atoms are much less reactive toward hydrogen-containing molecules than $\text{O}(^3\text{P})$.

The $\text{OH}(v=0$ and 1) decays were fitted (solid lines through measured concentrations in Figures 2 and 3) to exponential functions in a nonlinear least squares procedure for photolysis–probe delays greater than 18 μs to determine the decay rates. The decay of the $\text{OH}(v=0)$ concentration with the discharge off (Figure 2a) was fitted to a first-order decay rate of $452 \pm 30 \text{ s}^{-1}$. This observed loss rate mainly results from diffusion out of the probe laser beam, as well as a contribution from reactions of $\text{OH}(v=0)$ with H_2O_2 and photolytically produced radicals, in particular HO_2 . To determine the diffusion loss rate, the observed $\text{OH}(v=0)$ loss rate was compared with the results of kinetic modeling, as we did in our study of the collisional relaxation of $\text{OH}(v=1)$ by $\text{O}(^3\text{P})$ atoms.²⁰ Table 1 of ref 20 presents the processes included in the model. We derive a diffusion loss rate of $307 \pm 30 \text{ s}^{-1}$ for $\text{OH}(v=0)$. This value is within the experimental uncertainties of the value determined in our study of relaxation by $\text{O}(^3\text{P})$ atoms.²⁰ This loss was included in the analysis of the decay of $\text{OH}(v=0$ and 1) concentrations with the microwave discharge on.

Table 1 presents the determined $\text{OH}(v=0)$ decay rates in various runs with the microwave discharge on, listed in order

TABLE 1: OH($\nu=0$ and 1) Decay Rates and the Determination of $N(^4S)$ Concentrations^a

| OH($\nu=0$) decay rate (10^3 s^{-1}) | derived $[N(^4S)]$ ($10^{13} \text{ atoms cm}^{-3}$) | OH($\nu=1$) decay rate (10^4 s^{-1}) |
|--|--|--|
| 0.452 ± 0.030 | 0^b | 0.359 ± 0.028 |
| 1.630 ± 0.062 | 2.37 ± 0.17 | 0.746 ± 0.058 |
| 1.630 ± 0.062 | 2.37 ± 0.17 | 0.877 ± 0.112 |
| 1.630 ± 0.062 | 2.37 ± 0.17 | 0.703 ± 0.026 |
| 3.332 ± 0.048 | 5.92 ± 0.17 | 0.803 ± 0.074 |
| 3.337 ± 0.108 | 5.93 ± 0.26 | 1.049 ± 0.077 |
| 3.452 ± 0.049 | 6.17 ± 0.17 | 0.718 ± 0.089 |
| 3.941 ± 0.059 | 7.19 ± 0.19 | 0.880 ± 0.093 |
| 3.941 ± 0.059 | 7.19 ± 0.19 | 0.888 ± 0.142 |
| 4.003 ± 0.041 | 7.32 ± 0.17 | 1.146 ± 0.285 |
| 4.003 ± 0.041 | 7.32 ± 0.17 | 1.137 ± 0.250 |
| 4.677 ± 0.075 | 8.72 ± 0.22 | 1.279 ± 0.067 |
| 4.677 ± 0.075 | 8.72 ± 0.22 | 1.370 ± 0.108 |
| 4.969 ± 0.069 | 9.33 ± 0.22 | 0.93 ± 0.12 |
| 4.969 ± 0.069 | 9.33 ± 0.22 | 0.939 ± 0.075 |
| 7.996 ± 0.111 | 15.64 ± 0.33 | 1.39 ± 0.11 |
| 8.250 ± 0.095 | 16.17 ± 0.32 | 2.11 ± 0.21 |

^a Quoted uncertainties are 1σ . ^b Microwave discharge off.

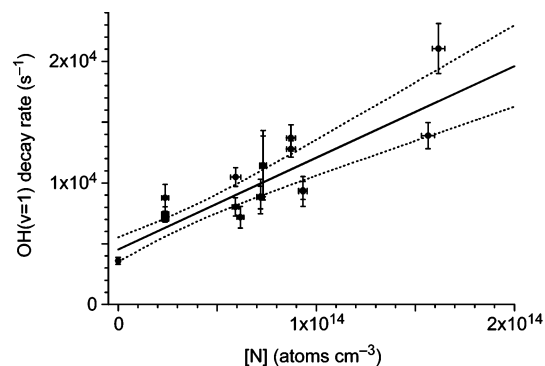


Figure 4. Plot of the determined OH($\nu=1$) decay rate with the microwave discharge on as a function of the $N(^4S)$ atom concentration, as determined from the measured OH($\nu=0$) decay rates. The plotted error bars are 1σ uncertainties. The 95% confidence limits on the fitted line are indicated with dotted lines.

of increasing decay rate, and hence increasing $N(^4S)$ concentration. These decay rates were employed to compute the $N(^4S)$ concentrations, using $k_{\nu=0}(\text{OH}-\text{N}) = 4.74 \times 10^{-11} \text{ cm}^3 \text{ molecule}^{-1} \text{ s}^{-1}$, from Howard and Smith.³⁵ To account for the small effect of diffusion and reactions other than $\text{OH} + N(^4S)$ involving $\text{OH}(\nu)$, the measured time-dependent $\text{OH}(\nu)$ concentrations were compared with a full kinetic modeling of species concentrations, using the rate constants listed in table 1 of ref 20, supplemented with $k_{\nu=0}(\text{OH}-\text{N})$ given above and the rate constant $k_{\nu=1}(\text{OH}-\text{N}_2) = 1.5 \times 10^{-15} \text{ cm}^3 \text{ molecule}^{-1} \text{ s}^{-1}$ for vibrational relaxation of $\text{OH}(\nu=1)$ by N_2 .¹⁷ The assumed N_2 dissociation fraction was varied in the kinetic model to match the measured decay rates. The derived values of the $N(^4S)$ concentrations are listed in Table 1 for each run. The estimated uncertainties in $[N(^4S)]$ includes fitting uncertainties, but not the uncertainty in the value of $k_{\nu=0}(\text{OH}-\text{N})$ employed³⁵ in the model.

The fitted decay rates for the measured time-dependent $\text{OH}(\nu=1)$ concentrations with the microwave discharge on are listed in Table 1 for the various runs. Under these conditions, the decay of the $\text{OH}(\nu=1)$ concentration is primarily determined by collisional removal by $N(^4S)$ atoms, with a significant contribution due to vibrational relaxation by H_2O_2 . We see from Figure 4 that the $\text{OH}(\nu=1)$ decay rate increases with increasing $N(^4S)$ concentration, although there is significant scatter in the data. From the H_2O_2 partial pressure (2.5 mTorr) and our previously

estimated²⁰ rate constant $k_{\nu=1}(\text{OH}-\text{H}_2\text{O}_2) = (4.0 \pm 1.0) \times 10^{-11} \text{ cm}^3 \text{ molecule}^{-1} \text{ s}^{-1}$ for vibrational relaxation of $\text{OH}(\nu=1)$ by H_2O_2 , the contribution of relaxation by H_2O_2 to the overall $\text{OH}(\nu=1)$ decay rate is $3.2 \times 10^3 \text{ s}^{-1}$. The estimated variation in the H_2O_2 partial pressure (± 1 mTorr) could lead to a variation in the $\text{OH}(\nu=1)$ decay rate ($\sim \pm 1.3 \times 10^3 \text{ s}^{-1}$), which is less than the scatter in the data plotted in Figure 4. The scatter in the data is mainly due to the noise in the $\text{OH}(\nu=1)$ concentration profiles, because of the small size of the signals.

To determine a value for $k_{\nu=1}(\text{OH}-\text{N})$, we carried out an unweighted linear squares fit of the $\text{OH}(\nu=1)$ decay rates as a function of $[N(^4S)]$. Because the Q coefficient⁴⁶ was <0.01 , an unweighted fit was deemed more appropriate than a weighted fit. We obtain a value $k_{\nu=1}(\text{OH}-\text{N}) = (7.6 \pm 2.1) \text{ cm}^3 \text{ molecule}^{-1} \text{ s}^{-1}$ [95% confidence limits, including the uncertainty in the literature value³⁵ for $k_{\nu=0}(\text{OH}-\text{N})$]. Because $[N(^4S)]$ and $k_{\nu=1}(\text{OH}-\text{N})$ are determined by the $\text{OH}(\nu=0$ and 1) decay rates, respectively, the ratio of $k_{\nu=1}(\text{OH}-\text{N})$ to $k_{\nu=0}(\text{OH}-\text{N})$ is better determined than $k_{\nu=1}(\text{OH}-\text{N})$ itself. For this ratio, we obtain 1.61 ± 0.42 .

4. Discussion

Although the uncertainty in the rate constant $k_{\nu=1}(\text{OH}-\text{N})$ is large, we find that there is a definite enhancement in the total removal rate constant for OH in collisions with $N(^4S)$ atoms when the radical is promoted to the $\nu=1$ vibrational level. This behavior contrasts with the slight increase, but within the experimental uncertainties, in the $\text{OH}-\text{O}(^3\text{P})$ total removal rate constant when the OH radical is promoted to the $\nu=1$ vibrational level.²⁰

As noted in the Introduction, $\text{OH}(\nu=0)$ radicals are removed by reaction only, whereas $\text{OH}(\nu=1)$ can be removed by reaction and, to a lesser extent, by vibrational relaxation, in collisions with $N(^4S)$ atoms. Because both chemical reaction and vibrational relaxation proceed predominantly through formation and decay of a transient HNO complex (see Figure 1),^{39,40} we can estimate the branching ratio for chemical reaction vs vibrational relaxation with a statistical theory, and we employ the prior distribution⁴⁷ here. Summing over the accessible rovibrational molecular levels, we find that the prior statistical model predicts branching ratios of 97 and 3% for chemical reaction and collisional vibrational relaxation, respectively, in $\text{OH}(\nu=1) + N(^4S)$ collisions. Thus, the main removal process in $\text{OH}(\nu=1)-N(^4S)$ collisions is predicted to be chemical reaction.

As discussed in the Introduction, the interaction of OH with $N(^4S)$ atoms is initially mediated through the strongly attractive $^3A''$ PES, leading to the transient formation of the HON complex. Three other PES's ($^3A'$, $^5A'$, $^5A''$) emanate from the $\text{OH}(^2\Pi) + N(^4S)$ asymptote, but these surfaces are repulsive.⁴⁸ The observed enhancement of the $k_{\nu}(\text{OH}-\text{N})$ rate constant with vibrational excitation of the OH radical suggests that the initial formation rate of the HON complex is accelerated and that this increased formation rate reflects the dependence of the $^3A''$ PES on the OH internuclear separation in the entrance channel. In the calculation of the ab initio points to describe the $\text{OH} + \text{N}$ $^3A''$ PES,^{34,49} the OH internuclear separation $R(\text{O}-\text{H})$ was fixed, and the dependence on this coordinate was not explicitly investigated. Hence, the dependence of the fitted $^3A''$ PES on $R(\text{O}-\text{H})$ may not be accurately described.

In their time-dependent quantum mechanical calculations on the $\text{OH} + N(^4S)$ reaction, Chen et al.⁴⁰ investigated the dependence of the reaction probability upon internal excitation of the OH radical. They did not observe a significant increase

in the reaction probability with excitation of OH to the $v=1$ or 2 vibrational levels for total angular momentum $J=0$. In view of the fact that the prior statistical theory predicts only a small branching ratio for vibrational relaxation of OH($v=0$), their neglect of this channel does not explain their observed negligible dependence of the reaction probability on the OH vibrational quantum number. It would be interesting to carry out a further theoretical investigation of this system, with explicit consideration of the dependence of the OH–N interaction energies upon the O–H internuclear separation.

Acknowledgment. We are grateful to Millard Alexander for his encouragement and for providing us with a copy of ref 23. Correspondence with George Schatz is also kindly acknowledged. This research has been supported by the Air Force Office of Scientific Research under grant no. FA9550-04-1-0103.

References and Notes

- (1) Atkinson, R.; Baulch, D. L.; Cox, R. A.; Crowley, J. N.; Hampson, R. F.; Hynes, R. G.; Jenkins, M. E.; Rossi, M. J.; Troe, J. *Atmos. Chem. Phys.* **2004**, *4*, 1461 (<http://www.iupac-kinetic.ch.cam.ac.uk/index.html>).
- (2) Sander, S. P.; Ravishankara, A. R.; Golden, D. M.; Kolb, C. E.; Kurylo, M. J.; Huie, R. E.; Orkin, V. L.; Molina, M. J.; Moortgat, G. K.; Finlayson-Pitts, B. J. *Chemical kinetics and photochemical data for use in atmospheric studies. Evaluation no. 14*; Jet Propulsion Laboratory: Pasadena, CA, 2003 (<http://jpldataeval.jpl.nasa.gov>).
- (3) Adler-Golden, S. J. *Geophys. Res.* **1997**, *102*, 19969.
- (4) McDade, I. C. *Adv. Space Res.* **1997**, *19*, 6653.
- (5) Conway, S. R.; Summers, M. E.; Stevens, M. H.; Cardon, J. G. *Geophys. Res. Lett.* **2000**, *27*, 2613.
- (6) Smith, I. W. M.; Williams, M. D. *J. Chem. Soc., Faraday Trans. 2* **1985**, *81*, 1849.
- (7) Raiche, G. A.; Jeffries, J. B.; Rensberger, K. J.; Crosley, D. R. *J. Chem. Phys.* **1990**, *92*, 7258.
- (8) Sappety, A. D.; Copeland, R. A. *J. Chem. Phys.* **1990**, *93*, 5741.
- (9) Dodd, J. A.; Lipson, S. J.; Blumberg, W. A. M. *J. Chem. Phys.* **1991**, *95*, 5752.
- (10) Chalamata, B. R.; Copeland, R. A. *J. Chem. Phys.* **1993**, *99*, 5807.
- (11) Knutsen, K.; Dyer, M. J.; Copeland, R. A. *J. Chem. Phys.* **1996**, *104*, 5798.
- (12) Dyer, M. J.; Knutsen, K.; Copeland, R. A. *J. Chem. Phys.* **1997**, *107*, 7809.
- (13) Silvente, E.; Richter, R. C.; Hynes, A. J. *J. Chem. Soc., Faraday Trans.* **1997**, *93*, 2821.
- (14) Yamasaki, K.; Watanabe, A.; Kakuda, T.; Tokue, I. *J. Phys. Chem. A* **2000**, *104*, 9081.
- (15) Lacoursière, J.; Dyer, M. J.; Copeland, R. A. *J. Chem. Phys.* **2003**, *118*, 1661.
- (16) McCabe, D. C.; Brown, S. S.; Gilles, M. K.; Talukdar, R. K.; Smith, I. W. M.; Ravishankara, A. R. *J. Phys. Chem. A* **2003**, *107*, 7762.
- (17) D'Ottone, L.; Bauer, D.; Campuzano-Jost, P.; Fardy, M.; Hynes, A. J. *Phys. Chem. Chem. Phys.* **2004**, *6*, 4276.
- (18) Spenser, J. E.; Glass, G. P. *Int. J. Chem. Kinet.* **1977**, *9*, 97.
- (19) Marshall, J.; Kalogerakis, K. S.; Copeland, R. A. Laboratory measurements of OH($v=2$) collisional reactivation by oxygen atoms. American Geophysical Union Spring 2001 meeting, paper SA31A-21.
- (20) Khachatryan, A.; Dagdigian, P. *J. Chem. Phys. Lett.* **2005**, *415*, 1.
- (21) Varandas, A. J. C. *Chem. Phys. Lett.* **2004**, *396*, 182.
- (22) Barnes, P. W.; Sharkey, P.; Sims, I. R.; Smith, I. W. M. *Faraday Discuss.* **1999**, *13*, 167.
- (23) Atahan, S.; Alexander, M. H. *J. Phys. Chem. A*, in press.
- (24) Rackham, E. J.; Huarte-Larrañaga, F.; Manolopoulos, D. E. *Chem. Phys. Lett.* **2001**, *343*, 356.
- (25) Rackham, E. J.; Gonzalez-Lezana, T.; Manolopoulos, D. E. *J. Chem. Phys.* **2003**, *119*, 12895.
- (26) Alexander, M. H.; Rackham, E. J.; Manolopoulos, D. E. *J. Chem. Phys.* **2004**, *121*, 5221.
- (27) Yardley, J. T. *Introduction to Molecular Energy Transfer*; Academic: New York, 1980.
- (28) Smith, I. W. M. *J. Chem. Soc., Faraday Trans.* **1997**, *93*, 3741.
- (29) Dodd, J. A.; Singleton, S. M.; Miller, S. M.; Armstrong, P. S.; Blumberg, W. A. M. *Chem. Phys. Lett.* **1996**, *260*, 103.
- (30) Hwang, E. S.; Castle, K. J.; Dodd, J. A. *J. Geophys. Res.* **2003**, *108*, 1109.
- (31) Duff, J. W.; Sharma, R. D. *J. Chem. Soc., Faraday Trans.* **1997**, *93*, 2645.
- (32) Chase, M. W., Jr.; Davies, C. A.; Downey, J. R., Jr.; Frurip, D. J.; McDonald, R. A.; Syverud, A. N. *J. Phys. Chem. Ref. Data* **1985**, *1985*, supplement no. 1.
- (33) Ruscic, B.; Feller, D.; Dixon, D. A.; Peterson, K. A.; Harding, L. B.; Asher, R. L.; Wagner, A. F. *J. Phys. Chem. A* **2001**, *105*, 1.
- (34) Guadagnini, R.; Schatz, G. C.; Walch, S. P. *J. Chem. Phys.* **1995**, *102*, 774.
- (35) Howard, M. J.; Smith, I. W. M. *J. Chem. Soc., Faraday Trans. 2* **1981**, *77*, 997.
- (36) Smith, I. W. M.; Stewart, D. W. A. *J. Chem. Soc., Faraday Trans.* **1994**, *90*, 3221.
- (37) Brune, W. H.; Schwab, J. J.; Anderson, J. G. *J. Phys. Chem.* **1983**, *87*, 4503.
- (38) Smith, I. W. M.; Tuckett, R. P.; Whitham, C. J. *J. Chem. Phys.* **1993**, *98*, 6267.
- (39) Guadagnini, R.; Schatz, G. C.; Walch, S. P. *J. Chem. Phys.* **1995**, *102*, 784.
- (40) Chen, M.-D.; Tang, B.-Y.; Han, K.-L.; Lou, N.-Q.; Zhang, J. Z. *H. J. Chem. Phys.* **2003**, *118*, 6852.
- (41) Manatt, S. L.; Manatt, M. R. R. *Chem. Eur. J.* **2004**, *10*, 6540.
- (42) Turnipseed, A. A.; Vaghjiani, G. L.; Thompson, J. E.; Ravishankara, A. R. *J. Chem. Phys.* **1992**, *96*, 5887.
- (43) Myers, T. L.; Förde, N. R.; Hu, B.; Kitchen, D. C.; Butler, L. J. *J. Chem. Phys.* **1997**, *107*, 5361.
- (44) Jacobs, A.; Kleinermanns, K.; Kuge, H.; Wolfrum, J. *J. Chem. Phys.* **1983**, *97*, 3162.
- (45) Grunewald, A. U.; Gericke, K.-H.; Comes, F. J. *J. Chem. Phys.* **1988**, *89*, 345.
- (46) Press, W. H.; Flannery, B. P.; Teukolsky, S. A.; Vetterling, W. T. *Numerical Recipes: The Art of Scientific Computing*; Cambridge University Press: Cambridge, 1980; Section 14.2.
- (47) Levine, R. D.; Bernstein, R. B. *Molecular Reaction Dynamics and Chemical Reactivity*; Oxford University Press: New York, 1987.
- (48) Walch, S. P. *J. Chem. Phys.* **1990**, *93*, 8036.
- (49) AIP document no. PAPS JCPSA-102-774-59.